Experimental and numerical analysis of the unreinforced and reinforced notched timber beam by a screw

Van Dang Tran[1*], Dong Tran[2], Marc Oudjene[3]

[1]Division of Transportation, Faculty of Civil Engineering, Thuyloi University, Vietnam
[2]Division of Engineering Geology, Faculty of Bridge and Road Engineering, National University of Civil Engineering, Vietnam
[3]LERMAB, Lorraine University, France

Received 15 May 2018; accepted 1 August 2018

Abstract:

Timber is highly anisotropic. It behaves differently in diverse directions. Tension and compression perpendicular to the grain present a low strength with respect to the ones parallel to the grain. To compensate for the lack, the self-tapping screw is an excellent choice for reinforcing the timber. This paper focuses on the notched timber beam with the experimental and numerical results. In the first part, the experimental results of the unreinforced notched beams and the screw reinforced notched beams under bending load will be presented. The second part describes a numerical study in which a 3D finite element (FE) model and a fast FE model of the notched beam reinforced by a self-tapping screw are realised. In particular, the fast FE model is simplified with the use of the screw's model as a beam element having one translational degree of freedom. This model not only presents a good result in comparison with the experiment as well as the 3D FE model but also requires six times less computational times as compared to the 3D FE model.

Keywords: **cohesive zone, finite element method, self-tapping screw, timber behaviour.**

Classification number: **2.3**

Introduction

Timber structure is mainly used in construction due to its outstanding properties such as high resistance and stability, aesthetic and, in particular, environment-friendly. However, timber behaves weakly in the direction perpendicular to the grain. Hence, its performance in the direction should be optimised to obtain a good global resistance of the timber structure. Various techniques with the aim of increasing the strength of timber structures have been used. These include the use of elements made from timber, iron, steel, aluminium, concrete and the more recent laminated timber, epoxy resins fibber reinforced polymers (FRP). The performance of timber can be extended by adding the steel elements at zones where the timber is weak or the timber can be reinforced by the manufactured technique of gluing several timber lamellas such as the glued laminated timber and the cross-laminated timber. On the other hand, FRP is used because it has several advantages, such as being easily applicable and suitable for the strengthening of timber elements under bending, connections between different elements, local bridging where defects are present, confining local rupture and preventing crack opening. The other solution is the use of epoxy resins as adhesives for the strengthening of extremities of the beam, the filling of hollow sections due to biotic attack and the in situ strengthening of floor beams. However, all these methods require materials with high cost, which are not common, especially in Vietnam. Self-tapping screws become the first choice because of their economic advantages and comparatively easy handling. The European Standard EN 1995-1-1 [1] presents the requirements for self-tapping screws. The literature review shows that the

*Corresponding author: Email: tranvandang@tlu.edu.vn.

research works about reinforcement are mostly focused on testing reinforcement materials and the development of alternative methods [2-10]. Extremely less attention was paid to the calculation methods predicting the load-carrying capacity of reinforced structures and joints [11]. Therefore, the need for the development of design methods arises, as it is a key point to assess the strength and deformation properties of reinforced structures and joints.

The present paper describes the experimental results related to the reinforcement of a notched beam by screws and a simplified finite element model to simulate the global behaviour of self-tapping screw reinforcements in timber structural elements and joints. The numerical methodology has been applied successfully to simulate the load-slip behaviour of timber connections [12-14]. Here, it is presented and applied in the context of reinforcement of the notched spruce beams. The obtained results are compared with the experimental tests, showing good agreement.

Experimental results

Methodology

The beam specimens have been made from a spruce timber, which has an average density of 420 kg/m^3 at the moisture constant that fluctuated between 10% and 12%. The experimental tests consist of two sets of notched beams: unreinforced notched beams (Fig. 1A) and reinforced notched beams (Fig. 1B).

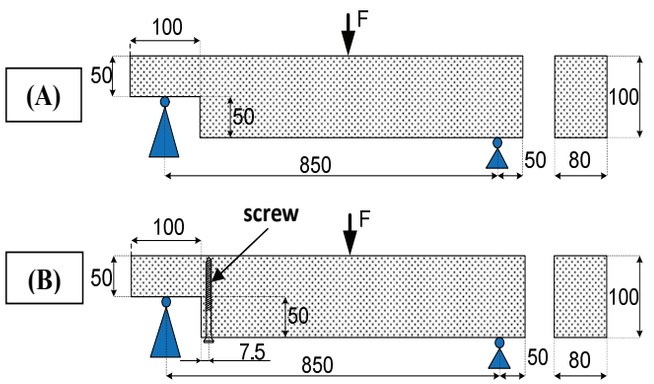

Fig. 1. Schematic illustration of the tested notched beams: (A) unreinforced beams, **(B)** reinforced beams.

The reinforced notched beam is reinforced by one screw at the perpendicular middle of the beam. As the reinforcement of the screw should impact as soon as the failure of the beam at the notch appears, the screw should be as near to the notch as possible (Fig. 2A).

The beams have a total length of 900 mm and a cross section of 100 mm x 80 mm. For the reinforcement of notches, a single threaded-screw of 100 mm length and 5 mm diameter was used (Fig. 2B).

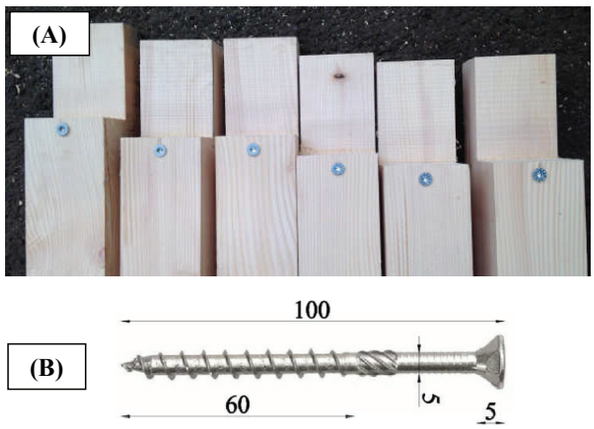

Fig. 2. Reinforced notched beams with one screw.

The specimens were tested under the three-point bending in a standard Instron machine (Fig. 3) with 150 kN load cell capacity at the crosshead speed of 2 mm/min.

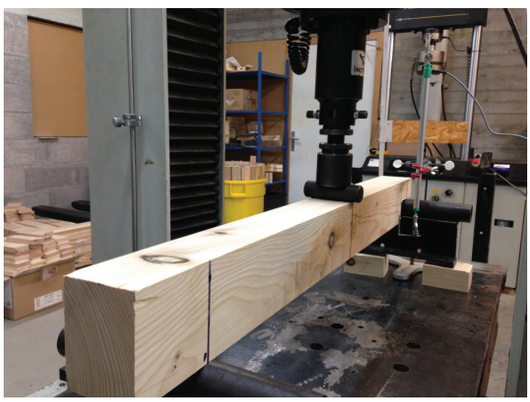

Fig. 3. Three-point bending test set-up.

Results

Fig. 4 and 5 display the experimental load-deflection curves from the unreinforced and the reinforced beams, respectively. Fig. 4 presents a brittle behaviour caused by the damage of timber in transversal tension at the notch. However, the curves from the reinforced beams in Fig.5 show a plastic behaviour after an initial elastic stage. The beams' performance in transversal tension is extended by the reinforcement of the screw. That causes the appearance of the elasto-plastic behaviour of the beams, and the damage initiates at a later stage. From these figures, it can be observed that the reinforced notches noticeably enhanced the load-carrying capacity of the entire beams.

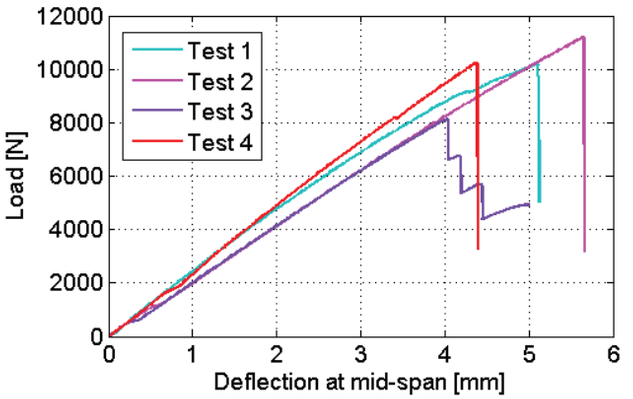

Fig. 4. Experimental load-deflection curves from the unreinforced beams.

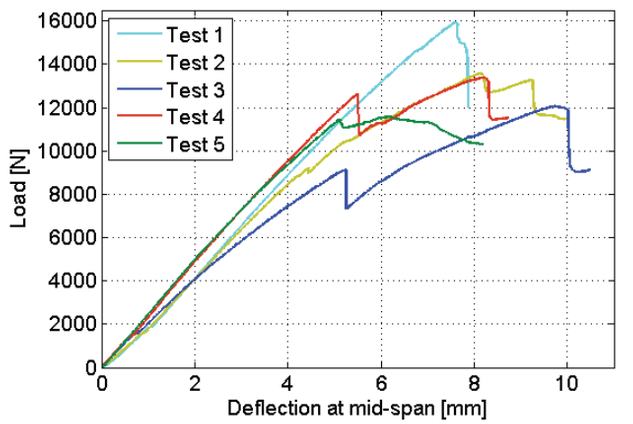

Fig. 5. Experimental load-deflection curves from the reinforced beams.

Additionally, the failure of the reinforced specimens shows less brittleness as compared to that of the unreinforced specimens. The load carrying capacity values recorded from all the beam specimens are summarised in Table 1, where it can be seen that the one-screw reinforcement has delayed the fracture of the notch details leading to the strengthening of the timber beams by about 34%.

Table 1. Experimental results of the reinforced notched beam and the unreinforced notched beam.

Tests N°	F_{max}(kN) Reinforced	F_{max}(kN) Unreinforced
1	15.97	10.17
2	13.57	11.21
3	12.07	08.13
4	13.37	10.22
5	11.58	/
Mean	**13.31**	**09.93**
C.o.V (%)	11.7	6.72

Modelling of the screw reinforcement

Mechanical behaviour of materials

Timber is a natural material. In the ideal model, timber can be considered as a homogeneous anisotropic material in three main directions: the longitudinal direction L (z), following the grain direction, the tangential direction T, corresponding with the tangent of the medullary ray, and the radial direction R, which is the centripetal direction (Fig. 6A, 6B).

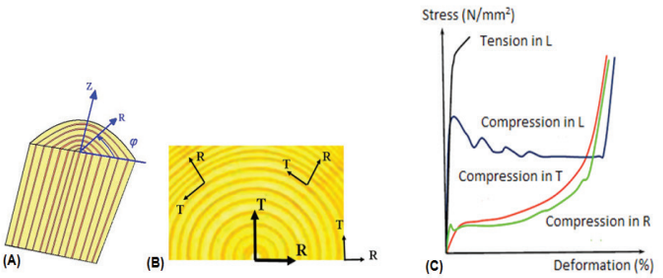

Fig. 6. (A) Longitudinal and radial direction; **(B)** Orthogonal direction: T and R; **(C)** Stress-deformation curve of timber in different directions.

The mechanical behaviour of timber in different directions is quite different. In tension according to the grain, the timber is crushed. In contrast, when it is compressed, the stress-strain curves appear as a flexible term to the endurance point. However, the strength of the wood subjected to the grain is significantly greater than that of compression in different directions (Fig. 6C).

The elastic behaviour is estimated by the Hooke's law, as follows:

$$\begin{pmatrix} \varepsilon_L \\ \varepsilon_R \\ \varepsilon_T \\ \gamma_{RT} \\ \gamma_{LT} \\ \gamma_{LR} \end{pmatrix} = \begin{bmatrix} 1/E_L & -\nu_{RL}/E_R & -\nu_{TL}/E_R & 0 & 0 & 0 \\ -\nu_{LR}/E_L & 1/E_R & -\nu_{TR}/E_T & 0 & 0 & 0 \\ -\nu_{LT}/E_R & -\nu_{RT}/E_R & 1/E_T & 0 & 0 & 0 \\ 0 & 0 & 0 & 1/2G_{RT} & 0 & 0 \\ 0 & 0 & 0 & 0 & 1/2G_{LT} & 0 \\ 0 & 0 & 0 & 0 & 0 & 1/2G_{LR} \end{bmatrix} \begin{pmatrix} \sigma_L \\ \sigma_R \\ \sigma_T \\ \tau_{RT} \\ \tau_{LT} \\ \tau_{LR} \end{pmatrix} \quad (1)$$

where, ε_I: deformations in the main directions (I = L, T, R); γ_{IJ}: angular deformations in the plans IJ (I, J = L, T, R); σ_I: nominal stresses following the direction I; τ_{IJ}: shear stresses in the plan IJ; E_I: Young's modulus according to the direction I; G_{IJ}: Coulomb's modulus according to the plan IJ; υ_{IJ}: Poisson's ratio according to the plan IJ.

The behaviour of plasticity initiates as soon as the stress reaches a threshold σ_e, called elastic limit and is expressed by a plastic criterion f_p.

The plastic criterion can be written by [15, 16]:

$$f_p = \|\underline{\sigma}\| - (R + \sigma_e) = 0; \quad R = \frac{Q}{b}\left(1 - e^{-b\Delta\lambda}\right) \tag{2}$$

where, $\|\underline{\sigma}\|$ is the standard of stress tensor; R is the stress of isotropic hardening; $\Delta\lambda$ is the cumulative deformation of plasticity; Q and b are the parameters of isotropic hardening.

The anisotropic plasticity is estimated by the Hill quadratic criterion [17]. The criterion assumes that the stress of isotropic hardening R is given by 0, so the equation (2) becomes as follows:

$$f_p = \|\underline{\sigma}\| - \sigma_e = 0 \Leftrightarrow \sqrt{\underline{\sigma} : \underline{\underline{H}} : \underline{\sigma}} - \sigma_e = 0$$

$$\Leftrightarrow \sqrt{F(\sigma_{22} - \sigma_{33})^2 + G(\sigma_{33} - \sigma_{11})^2 + H(\sigma_{11} - \sigma_{22})^2 + 2L\sigma_{23}^2 + 2M\sigma_{31}^2 + 2N\sigma_{12}^2} = \sigma_e \tag{3}$$

F, G, H, L, M, N are the Hill's constants, estimated as follows:

$$\sigma_L = \frac{\sigma_e}{\sqrt{G+H}}; \sigma_R = \frac{\sigma_e}{\sqrt{F+H}}; \sigma_T = \frac{\sigma_e}{\sqrt{G+F}}$$

$$L = \frac{\sigma_e^2}{2\tau_{RT}^2}; M = \frac{\sigma_e^2}{2\tau_{LT}^2}; N = \frac{\sigma_e^2}{2\tau_{LR}^2}$$

where, σ_L, σ_R, σ_T, are the threshold stress in compression according to the longitudinal, radial, tangential direction of the grain, respectively, as estimated by the experiment.
τ_{RT}, τ_{LT}, τ_{LR}, are the threshold stress in shear according to the plans RT, LT and LR, respectively, as estimated by the experiment.

During the bending test, the cracking initiates within the notch detail of the beams and propagates along the grain direction under the mode I crack growth. The bi-linear traction-separation law was adequately used for the mode I crack growth [18]. The parameters of the traction-separation law to simulate cracking of timber under mode I have been determined with an appropriate experimental procedure based on the modified DCB test similar to that used in [19, 20].

The linear traction-separation law is assumed to compose of three states: the first is the linear elastic behaviour, the second is the initiation of the damage and then, the last is the evolution of the damage (Fig. 7).

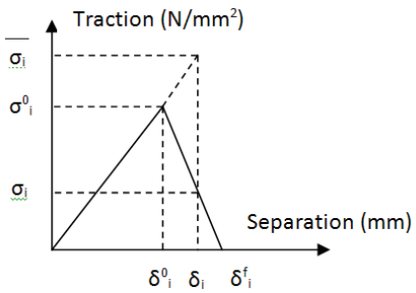

Fig. 7. Traction-separation behaviour.

The elastic behaviour can be estimated as follows:

$$\begin{pmatrix} \sigma_n \\ \sigma_t \\ \sigma_s \end{pmatrix} = \begin{bmatrix} K_{nn} & K_{nn} & K_{nn} \\ K_{nn} & K_{nn} & K_{nn} \\ K_{nn} & K_{nn} & K_{nn} \end{bmatrix} \begin{pmatrix} \delta_n \\ \delta_t \\ \delta_s \end{pmatrix} \tag{4}$$

where, σ_n, σ_s and σ_t represent the stresses in the normal and tangential directions, respectively. δ_n, δ_s and δ_t are the relative displacements (separations) in the normal and tangential directions, respectively. K_{ij} is the rigidities in the plan ij (i, j = n, s, t).

The quadratic maximum stress is selected to evaluate the initiation of damage, as follows:

$$\left(\frac{\sigma_n}{\sigma_n^c}\right)^2 + \left(\frac{\sigma_s}{\sigma_s^c}\right)^2 + \left(\frac{\sigma_t}{\sigma_t^c}\right)^2 = 1 \tag{5}$$

where, σ_n^c, σ_s^c and σ_t^c are the maximum stresses according to the nominal and transversal directions.

The evolution of the damage is assumed to be a linear displacement-based softening:

$$\sigma_n = \begin{cases} (1-D)\overline{\sigma_n} \Leftrightarrow \overline{\sigma_n} \geq 0 \\ \overline{\sigma_n} \Leftrightarrow \overline{\sigma_n} < 0 \end{cases}$$
$$\sigma_n = (1-D)\overline{\sigma_s} \tag{6}$$
$$\sigma_n = (1-D)\overline{\sigma_t}$$

where, D is a scalar damage variable, which allows the simulation of the degradation of the cohesive stiffness. It is evaluated by a function of the effective separation as follows:

$$D = \frac{\delta_m^f\left(\delta_m^{\max} - \delta_m^0\right)}{\delta_m^{\max}\left(\delta_m^f - \delta_m^0\right)}$$
$$\delta_m = \sqrt{(\delta_m)^2 + (\delta_s)^2 + (\delta_t)^2} \tag{7}$$

where, δ_m^0 and δ_m^f is the effective displacement at the initiation and ending moment of the damage, respectively; δ_m^{max} is the maximum effective displacement during charging history.

Numerical approach and Finite element models

The behavior of the contact between the screw and the timber is described by three internal forces: tension, shearing and bending (Fig. 8). In this, the shearing and the bending are due to the contact between two bodies of timber. The tension is caused by the contact between the screw and the timber such as the screw-head embedment and the friction between the screw and the timber. In relation to the tension, if the friction between the screw and timber is neglected, the remaining force will be due to the screw-head embedment.

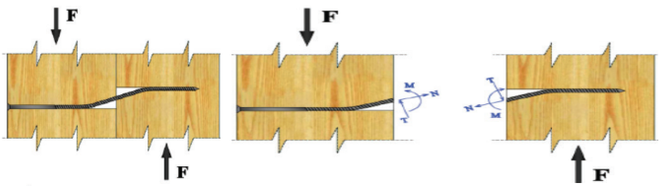

Fig. 8. Internal forces of the reinforced screw.

The basic idea is to build a model with the beam element for the screw's part and the 3D solid element for the timber's part (Fig. 9). However, the problem is the incompatibility of the degree of freedom (dof) between the beam element and the solid element. Therefore, the 2-node beam element has to modified to obtain a modified element beam with only translational dof, which is compatible with the solid element [14]. In this model, the element beam is coupled to the mesh of the solid timber element. The approach has been earlier validated in the context of timber-to-timber and timber-to-concrete connections [12, 13]. Here, it is applied in the context of timber reinforcement based on full continuity between screw and timber similar to steel reinforcement in concrete structures.

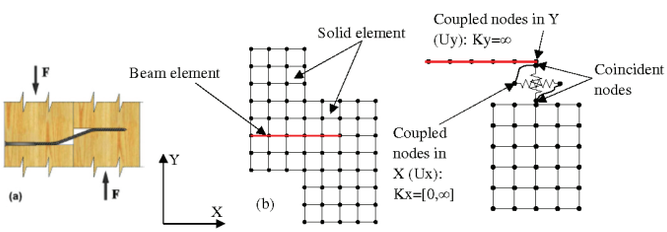

Fig. 9. Beam-to-solid element approach of the reinforced timber by screw.

In order to demonstrate the main advantages of the proposed approach, the simulation of the reinforced beams was undertaken in two ways:

- Model 1: both the screws and the timber beams have been modelled using 3D constitutive laws involving brick-solid element meshes (Fig. 10A).

- Model 2: the timber beam was simulated using 3D constitutive law, whereas the screw was modelled using a one-dimensional beam element (Fig. 10B), leading to a beam-to-solid coupling (proposed approach).

Note that the first model (Model 1) is not efficient in the case of large number of screws. In order to reduce the computational time, only one half of the model was simulated, sine the symmetry of the model (Fig. 10).

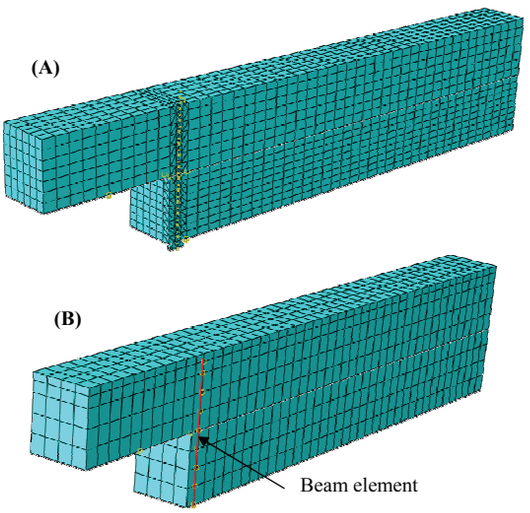

Fig. 10. Finite element meshes (one half) of the notched beams: (A) Model 1; **(B)** Model 2.

For the timber, the 8-node solid element was used. Orthotropic-anisotropic non-linear material model [15, 16, 20-23] has been assumed for the timber behaviour. The mechanical properties of timber are shown in Table 2.

Table 2. Elasto-plastic properties of timber.

Elasticity	Plasticity
E_L = 10000 MPa	f_L = 25 MPa
$E_R = E_T$ = 490 MPa	$f_R = f_T$ = 2.9 MPa
$\upsilon_{LR} = \upsilon_{LT}$ = 0.41	f_{RT} = 5.5 MPa
Y_{RT} = 0.33	σ_e = 25 MPa
$G_{LR} = G_{LT}$ = 650 MPa G_{RT} = 100 MPa	Q = 10 MPa; b = 2.5 F = 73,8; G = H = 0.5 N = M = L = 10.3

To simulate the mode I crack growth in timber, the cohesive zone model (CZM), exhibited in ABQAUS, is used, with the optimal damage parameters summarised in Table 3.

Table 3. The optimal damage parameters of the mode I crack growth.

Stiffness (N/mm^3)	Failure stress (N/mm^2)	Total failure displacement (mm)
$K_{nn} = 2$	$\sigma_n^c = 0.9$	$\delta_m^f = 0.02$

The isotropic elasto-plastic behaviour is used for the screw material and modelled using the modified one-dimensional beam element. The elastic modulus of the screw is selected as $E_s = 210$ GPa and its yield strength is $\sigma_y = 400$ N/mm^2. The nodes of the element beam of the screw and the corresponding nodes of the solid element of the timber were coupled with the constraint condition.

Results and discussion

The numerical simulation of the unreinforced notched beams has been undertaken, and the results were compared with the experiment. It can be seen that the numerical load-deflection curve fits well with the experimental curve (Fig. 11). Thus, it can be concluded that the CZM can adequately simulate the progressive cracking of the timber under opening fracture mode. Fig. 12 displays the comparison between the numerical and the experimental failure modes, which shows a good correlation.

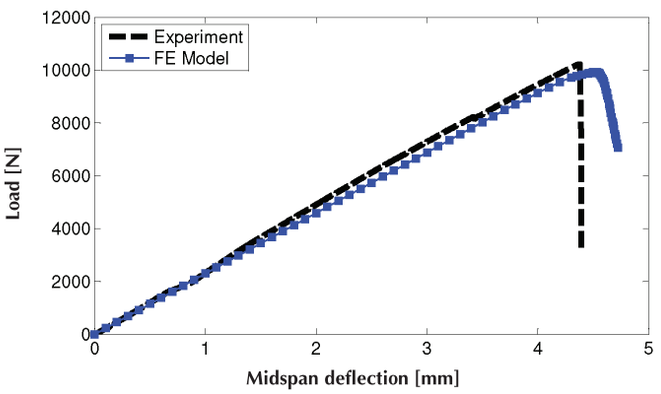

Fig. 11. Comparison between numerically predicted load-deflection curve and experimental curves from unreinforced beams.

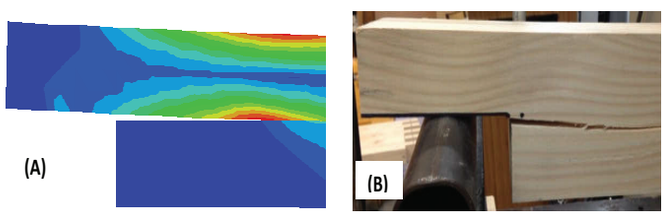

Fig. 12. Failure of the notch detail: (A) FE model, **(B)** experiment.

Figure 13 shows the numerically predicted load-deflection curves against experimental ones. It can be seen that both Model 1 and Model 2 perfectly predict the global response of the reinforced specimens including the progressive failure of the notches.

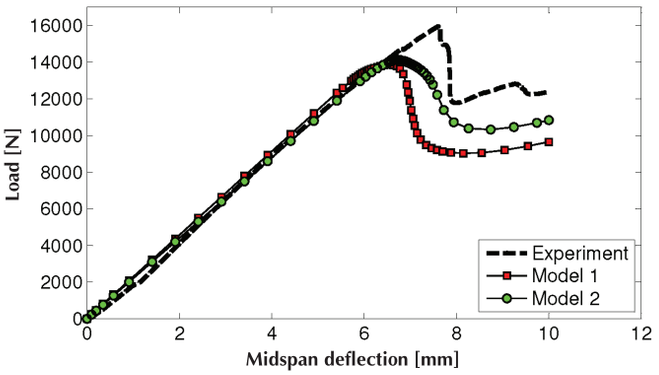

Fig. 13. Comparison between numerically and experimentally predicted load-deflection curves.

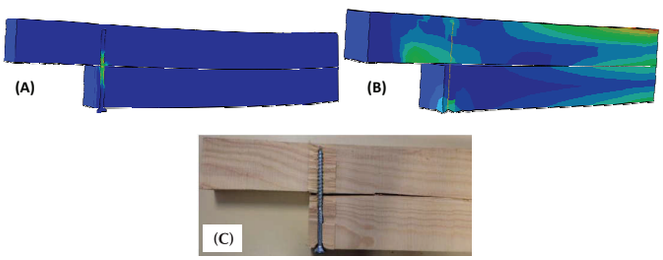

Fig. 14. Comparison between numerically and experimentally predicted failure modes: (A) Model 1, **(B)** Model 2, **(C)** Experiment.

Figure 14 illustrates the experimental mode of failure as well as those predicted by the numerical simulations, where a good correlation can be observed. Both the models show good and similar quality results; however, Model 2 has shown a higher amount of simplicity and quickness, as it requires six times less computational time as compared to Model 1.

Conclusions

This paper presents a simple method for reinforcing the timber structure in using the screws. The research is focused on the notched beam. Two sets of unreinforced and reinforced notched beams have been carried out, in order to find out the mechanism of this structure. Effectively, the notched beam reinforced by a screw shows 34% gain when compared with the unreinforced beam. Through the experiment, it seems that the failure mode of the notched beam is similar to the mode I crack growth. Therefore, in the numerical part, the finite element models were realised, using the cohesive behavior, to simulate the behavior of

the unreinforced notched beam and the reinforced notched beam by a screw. The results present a good correlation in comparison with the experiment. In particular, a fast finite element model has been established, using a beam element with one translational degree of freedom for the screw's model, which allows the reduction of the computational time by six times as compared to the full 3D model.

REFERENCES

[1] European Committee for Standardization EN 1995-1-1:2004+A1 (2008), *Eurocode 5: Design of timber structures - part 1.1: General - common rules and rules for buildings.*

[2] A. Kevarinmäki (2002), "Joints with inclined screws", *Proceeding CIB-W18/35-7-5,* Kyoto, Japan.

[3] F. Prat-Vincent, C. Rogers, et al. (2010), "Evaluation of the performance of joist-to header selftapping screw connections", *World Conference on Timber Engineering*, Trentino, Italy.

[4] P. Ellingsbø, K.A. Malo (2012), "Withdrawal Capacity of Long Self-Tapping Screws Parallel to Grain Direction", *World Conference on Timber Engineering*, Auckland.

[5] P. Mestek, H. Kreuzinger, S. Winter (2011), "Design concept for CLT - reinforced with Self-tapping screws", *Proceeding of CIB-W18/*44-7-6, Alghero, Italy.

[6] S. Franke, B. Franke, A.M. Harte (2015), "Failure modes and reinforcement techniques for timber beams - state of the art", *Construction and Building Materials*, **97**, pp.2-13.

[7] P. Dietsch, R. Brandner (2015), "Self-tapping screws and threaded rods as reinforcement for structural timber elements - A state of the art", *Construction and Building Materials*, **97**, pp.78-89.

[8] H.J. Blaß, M. Frese (2012), "Failure analysis on timber structures in Germany", *Lehrstuhl für Ingenieurholzbau und Baukonstruktionen*, Universität Karlsruhe, Germany, doi:10.1016/j.engstruct.2011.02.030.

[9] H.J. Blaß, P. Schädle (2011), "Ductility aspects of reinforced and non-reinforced timber joints", *Engineering Structures*, **33**, pp.3018-3026.

[10] A.M. Harte, K. Crews (2015), "Special issue: Reinforcement of timber structures", *Construction and Building Materials*, **97,** pp.1-130.

[11] R. Tomasi, A. Crosatti, et al. (2010), "Theoretical and experimental analysis of timber-to-timber joints connected with inclined screws", *Construction and Building Materials,* **24**, pp.1560-1571.

[12] E.M. Meghlat, M. Oudjene, H. Ait-Aider, J.L. Batoz (2013), "A new approach to model nailed and screwed timber joints using the finite element method", *Construction and Building Materials,* **41**, pp.263-269.

[13] M. Oudjene, E.M. Meghlat, H. Ait-Aider, J.L. Batoz (2013), "Non-linear finite element modelling of the structural behavior of screwed timber-to-concrete composite connections", *Composite Structures,* **102**, pp.20-28.

[14] Meghlat, E.M. Oudjene, M. Ait-Aider, H. Batoz, J.L. Batoz (2012), "A one-dimentional 4-node shear-flexible beam element for beam-to-solid modelling in mechanically jointed connections made with screws or nails", *ECCOMAS 2012 - European Congress on Computational Methods in Applied Sciences and Engineering*, e-Book Full Papers.

[15] M. Oudjene, M. Khelifa (2009), "Finite element modelling of wooden structures at large deformations and brittle failure prediction", *Materials and Design*, **30**, pp.4081-4087.

[16] M. Oudjene, M. Khelifa (2009), "Elasto-plastic constitutive law for wood behavior under compressive loadings", *Construction Building Materials*, **23**, pp.3359-3366.

[17] R. Hill (1948), *A theory of yielding and plastic flow of anisotropic metals*, Royal Soc. Lond. Proc., p.281.

[18] Abaqus theory manual (2008), *Dassault Systemes Simulia Corp. Providence: Rhode Island*, U.S.A.

[19] S. Fortino, G. Zagari, A.L. Mendicino, G. Dill-Langer (2012), "A simplified approach for FEM simulation of mode I cohesive crack growth in glued laminated timber under short-term loading", *J. Struct. Mech.*, **45**, pp.1-20

[20] Van-Dang Tran, Marc Oudjene, Pierre-Jean Méausoone (2014), "FE analysis and geometrical optimization of timber beech finger-joint under bending test", *International Journal of Adhesion and Adhesives*, **52**, pp.40-47.

[21] M. Oudjene, M. Khelifa (2010), "Experimental and numerical analyses of single double shear dowel-type timber joints", *Proceedings of the 11th World Conference on Timber Engineering.*

[22] C. O'Loinsigh, M. Oudjene, E. Shotton, A. Pizzi, P. Fanning (2012), "Mechanical behavior and 3D stress analysis of multi-layered wooden beams made with welded-through wood dowels", *Composite Structures*, **94**, pp.313-321.

[23] M. Oudjene, M. Khelifa, C. Segovia, A. Pizzi (2010), "Application of numerical modelling to dowel-welded wood joints", *J. Adhes.Sci.Technol.*, **24**, pp.359-70.